THE NATURE OF THE HELICAL GROOVE ON THE TOBACCO MOSAIC VIRUS PARTICLE

X-RAY DIFFRACTION STUDIES

by

ROSALIND E. FRANKLIN AND A. KLUG

Birkbeck College, Crystallography Laboratory, University of London (England)

1. INTRODUCTION

It is well known that the particles of tobacco mosaic virus (TMV) are rods of diameter about 150 A[1] and length about 3000 A[2]. In spite of extensive studies in many laboratories, the use of the electron microscope has not established the existence of any definite surface structure, or regular deviation from cylindrical form, in TMV particles. Short fragments of the particles, however, tend to show a hexagonal cross-section[3]. The purpose of this paper is to present evidence, derived from X-ray diffraction measurements, indicating that the TMV particle is neither a smooth cylinder nor a hexagonal prism, but rather a rod bearing either a helical groove or a helical array of protuberances.

Recent X-ray diffraction studies of TMV[4,5] have indicated that the virus protein is composed of structurally equivalent units, or sub-molecules, set in helical array around the long axis of the particle. The pitch of the helix on which the protein units lie is 23 A. The identity (or near-identity[6]) period of the structure in the direction of the long axis of the particle is 69 A, there being (to a close approximation[6]) $3n + 1$ protein units on 3 turns of the helix. It has already been suggested[5] that an important feature of the structure is an external groove following the line of the main protein helix. More detailed information about the nature of this groove has now been obtained from a further examination of X-ray fibre-diagrams of TMV gel, and also from a comparison of these diagrams with those given by dry orientated TMV.

Several independent lines of evidence confirm the existence of some kind of helical grooving of the TMV particle. The depth of the groove is estimated to be about 30 A, and its shape must be such as to permit a high degree of interlocking when parallel virus particles are brought into contact with one another.

A helical groove implies the existence of a helical ridge. This ridge, however, maywell be serrated rather than continuous and smooth. The serrations may, in fact, be such as to reduce the ridge to a helical array of protuberances, each protuberance corresponding to one protein sub-unit.

A particle of such a shape obviously has a more extensive surface than an equivalent cylindrical particle. Since the (mean) radius of the TMV particle is only

References p. 416.

about 75 A, and, of this, the RNA core must occupy the inner 15–20 A[4,7,8], it is clear that a substantial part of the virus protein must lie in the proximity of the surface. This may well be of considerable importance in determining the chemical activity of the virus.

2. ASPECTS OF THE THEORY OF DIFFRACTION BY HELICAL STRUCTURES

Before presenting the evidence for the existence of the groove and describing the methods by which its depth can be estimated, it will be necessary to summarise some results of the theory of X-ray diffraction by helical structures[9].

A helical molecule consists of atoms arranged on a number of constituent coaxial helices of varying radii and azimuth, each set of structurally equivalent atoms in the molecule being uniformly distributed along one such helix. If the helical molecule is built up of sub-units which are chemically and structurally identical, these sub-units lying in helical array around the molecular axis, there will be one constituent helix for each atom of the sub-unit. It is important to note that, in such a structure each constituent helix of the molecule must be of the same pitch and bear the same number of atoms. The radius and azimuth and the z co-ordinate of the first atom will, of course, vary.

(a) We shall first see what happens when the helical character of the molecule is retained but no account is taken of the fact that the structure ultimately consists of discrete atoms. That is, we shall consider the total electron density of the atoms lying on any one helix to be "smoothed" along it to give a line helix of uniform density.

Now the scattering function, or Fourier transform, of such a set of smooth, thin helices of radii r_i and all of pitch P is finite only on a series of layer-lines whose spacing is n/P (n integer). On the nth layer-line it takes the form (using cylindrical co-ordinates r, φ, z in real space and R, ψ, ζ in reciprocal space)

$$F_n = \sum_i J_n (2\pi R r_i) \exp [in (\psi + \tfrac{1}{2}\pi)]$$

where J_n is the Bessel function of order n. The distance R_1, of the first peak in $J_n (2\pi rR)$ from the axis of the transform is inversely proportional to r; for a given value of r, it is inversely proportional to n. Contributions from the different helices interfere with one another. The innermost maxima on each layer-line, however, will be due, in general, to the helices of largest radii. It is to be noted that on any one layer line there are contributions from Bessel functions of one order only. This is shown diagrammatically in Fig. 1a in which the order of Bessel function is plotted against the layer-line number.

(b) Now consider each of the simple, smooth helices of 2(a) to be replaced by a series of equally spaced point scatterers (or atoms) lying on it. Let the spacing of these atoms in the direction of the helical axis be p. The scattering function of this structure consists of the transform of the smooth, thin helices of 2(a) repeated throughout reciprocal space at intervals of $1/p$ in the axial direction.

If there is a whole number of inter-atomic axial spacings, p, in one turn of the helix (P/p integer), then the new origins of the transform of the smooth helices, which now occur at intervals of $1/p$ in the axial direction, will all fall on layer-lines

References p. 416.

of the original transform (*i.e.* at the spacings n/p). But each layer-line will now be contributed to by parts of the scattering function emanating from a number of different origins, and therefore by Bessel functions of a number of different orders. The orders occurring on any layer-line are shown in Fig. 1b. In general, only the contributions from the lower order Bessel functions will be appreciable. More important for our purposes is the fact that for small values of the layer-line index l, the lowest order Bessel function occurring on the layer-line is that which corresponds to the case of smooth helices. This means that the regions around the centre of the X-ray fibre diagrams in the two cases will be identical (*cf.* Figs. 1a and 1b), and for discussions of this part of the scattering pattern, we may regard the constituent helices of the molecule as being smooth.

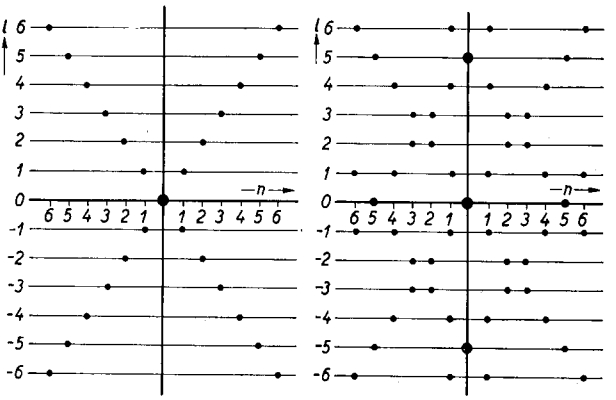

Fig. 1a. Diffraction by a smooth helix. Plot of the order n of the Bessel function contributing to the layer line l.
Fig. 1b. Discrete atoms on a helix. An (n, l) plot for the hypothetical case of 5 atoms per turn of helix. Note that the region near the origin is the same as in Fig. 1a.

(c) Before we can discuss the case of TMV, it remains to consider what happens when a helical molecule does not contain a whole number of sub-units in one turn of the helix.

If P/p is not an integer, scattering is no longer confined to the original set of layer lines. Suppose, however, that there is exactly (or very nearly exactly[9]) a whole number, u, of scattering units in t turns of the helix ($tP/p = u$), There will then be an axial repeat of spacing $c = tP = up$, and hence in reciprocal space layer-lines of spacing $1/c$. The total number of layer-lines will thus be increased t-fold. Of the series of new origins of the transform of the smooth helix (2a) which occur at intervals of $1/p$ in the axial direction, every t^{th} origin will be on one of the original layer-lines. Contributions emanating from the first origin will thus now appear on every t^{th} layer-line[9,6], and we must bear this in mind when discussing TMV in which t is 3 and u probably 37[5].

The above remarks (2b) about the relationship between the transforms of smoothed and of point helices still apply, but in this case it is the lowest order Bessel functions on the 3rd, 6th *etc.* layer-lines which are unchanged in passing from a smooth helix to one bearing discrete atoms. This is the result which is used in Section 7.

3. THE HELICAL STRUCTURE OF TMV PROTEIN

TMV protein is considered to be a helical molecule of the type described under (2c) above; both chemical and X-ray evidence indicate that the protein is composed of units which are identical or nearly so.

It was stated above that the axial repeat of 69 A contains 3 turns of the helix (*i.e.* in the above notation, $t = 3$). Since the whole of what follows is based on this

References p. 416.

conclusion, the principal evidence on which it was based will be summarised here.

If $t = 3$, each layer-line $3n$ will have a contribution from a Bessel function of order n. Since the Bessel functions which can be identified with the greatest ease and certainty are those of lowest order, we shall confine our attention to the 3rd and 6th layer-lines, which should have contributions of J_1 and J_2 respectively.

On both the 3rd and 6th layer-lines, the first intensity maximum lies close to but not at the centre. Moving out from the centre, each of these layer-lines shows a regular periodicity of intensity. From the period (and independently of the position) of the intensity maxima, it is possible to determine the radius on which lies that part of the structure principally contributing to the scattering in the region concerned. From the value, r, of the radius so determined, and the position, R_1, of the first intensity maximum, the order, n, of the Bessel function $J_n(2\pi rR)$ which has its first maximum at R_1 can be determined. In this way we find that for the 3rd layer-line $r = 77$ A and $n = 1$, and for the 6th layer-line $r = 55$ A and $n = 2$. The results are summarised in Table I.

TABLE I

	3rd layer line		*6th layer line*	
	R-values for positions of observed intensity maxima	*R-values for maxima of $J_1^2(2\pi Rr)$ when $r = 77$ A*	*R-values for positions of observed intensity maxima*	*R-values for maxima of $J_2^2(2\pi Rr)$ when $r = 55$ A*
1	0.0037	0.0038	0.0083	0.0105
2	0.0101	0.0110	0.0240	0.0231
3	0.0173	0.0176	0.0341	0.0345
4	0.0245	0.0242	0.0456	0.0455
5	0.0309	0.0307	0.0575	0.0565
6	—	0.0373	0.0671	0.0673
7	0.0428	0.0437	0.0773	0.0784
8	0.0505	0.0502		
9	0.0580	0.0568		
10	0.0651	0.0632		

These results show that the central regions of the 3rd and 6th layer-lines may be closely approximated by Bessel functions of the 1st and 2nd order respectively. It will be clear from the theoretical results given in the preceding section that this is very strong evidence both that the structure is helical and that it repeats itself after 3 turns of the helix.

We are naturally led to enquire whether the diffraction data could be explained in an alternative manner in terms of a structure built up by stacking of discs. Any helical structure which has a true axial repeat can, of course, be considered, formally, as a pile of discs of thickness equal to the aixal repeat distance. But the helical structure would still exist within each disc. Alternatively, the structure can be considered as a pile of thinner discs, each containing the equivalent of one building unit of the helix, and each rotated by a fixed angle with respect to its neighbours. Here the helical symmetry is given by the rotation of each disc with respect to its neighnours. The diffraction data cannot, however, be accounted for by any stacking of discs which does not introduce helical symmetry.

The helical nature of the structure of TMV protein has been discussed in greater detail elsewhere[6].

References p. 416.

4. THE THIRD LAYER-LINE: EVIDENCE FOR A HELICAL GROOVE

The central region of the 3rd layer-line of an X-ray diagram of a TMV gel shows a regular periodicity in the intensity, with a period corresponding to a radius of 77 A. (Table I). This effect is particularly marked in the mild strain U2[10] and is shown in Fig. 2.

The accepted radius of the TMV particle is 75 A. Thus it is the outermost shell of the particle which contributes strongly to scattering on the 3rd layer-line. It follows that there is, in the outermost shell, a very strong density fluctuation with a period equal to the pitch of the helix, 23 A. The simplest explanation of this is that the outside of the virus particle bears a groove which follows the line of the helix.

Fig. 2. The central region of the 3rd layer-line of a X-ray fibre diagram of TMV gel. The arrows point to the positions of the nodes in the intensity pattern.

It appears, from Fig. 2, that the small-period intensity oscillation discussed above is modulated by a function of larger period, having nodes near the positions indicated by arrows. It will now be shown that such a modulation function is a necessary consequence of a helical groove, and that the position of the nodes enables the depth of the groove to be estimated.

For this purpose it will be necessary first to derive the Fourier transform of a helically grooved rod.

5. THEORY OF DIFFRACTION BY A HELICALLY GROOVED ROD

The diffraction phenomena with which we are here concerned correspond to spacings greater than about 15 A. We shall thus, as a first approximation, ignore the fluctuations in scattering density due to the fact that the structure is composed of discrete atoms, and treat the case of diffraction by a cylinder of uniform density which bears a helical groove on its outer surface.

For an exact treatment it is necessary to assume a particular form for the contour of the axial section, or profile, of the groove. However, we shall show (see below) that certain important features of the diffraction pattern are independent of the groove profile chosen. We shall therefore discuss in detail only two forms of profile, the treatment of which is particularly simple.

(a) As a model of a helically grooved cylinder we shall first consider the volume swept out by a very thin disc of radius r_0 whose centre moves along a helix of radius δ and pitch P, the plane of the disc lying always perpendicular to the axis of the helix. It may be shown, that, if δ is small, the profile of the helical groove so formed is, to a first approximation, sinusoidal. The significance of r_0, δ and P is indicated in Fig. 3a.

In mathematical terms, this grooved cylinder is obtained by the *folding* (or *convolution*) of the disc of radius r_0 with the helix of radius δ. Thus, by a well-known theorem[11] the Fourier transform of the structure is given by the product of the individual transforms of the disc and helix.

References p. 416.

The transform of a disc of radius r_0 is independent of ζ and ψ and is given by:

$$\pi r_0^2 \frac{2 J_1 (2\pi R r_0)}{2\pi R r_0}$$

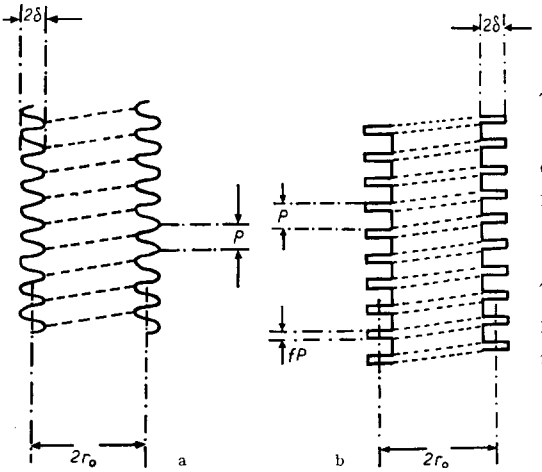

Fig. 3. Sections parallel to the axis of a uniform cylinder of mean radius r_0 which bears a helical groove of pitch P and of half-depth δ. (a) Quasi-sinusoidal groove profile; (b) Rectangular profile. f is the fraction of a period occupied by the ridge.

The transform of a thin helix of radius δ and pitch P is (see Section (2a)) finite only at values of $\zeta = n/P$ which are multiples of $1/P$, where it is of the form

$$J_n (2\pi\delta R)$$

The resulting product is thus also finite only on a series of layer lines n, where it has the value

$$\pi r^{02} \frac{2 J_1 (2\pi r_0 R)}{2\pi r_0 R} J_n (2\pi\delta R) \qquad (3)$$

per unit length of particle. The layer-lines n are those that correspond to the smooth continuous helix. Hence, following section (2c) above, we see that $n = 1$ corresponds to the 3rd layer-line in TMV, $n = 2$ to the 6th, and so on. $n = 0$ gives, of course, the equator of the diffraction pattern.

We shall be concerned only with the central regions of the equator and third layer line.

The equator

The transform is here

$$\pi r_0^2 \frac{2 J_1 (2\pi r_0 R)}{2\pi r_0 R} J_0 (2\pi\delta R) \qquad (4)$$

For very small values of R for which J_0 is close to unity, the expression approximates to the transform of a uniform cylinder of radius r_0. For larger values of R, the more slowly varying second factor J_0 will modulate the first, and the transform will differ from that of a simple cylinder.

The 3rd layer line

On the 3rd layer-line the transform has the value

$$\pi r_0^2 \frac{2 J_1 (2\pi r_0 R)}{2\pi r_0 R} J_1 (2\pi\delta R) \qquad (5)$$

which is again of the form of a rapidly varying function of period $1/r_0$ modulated by a function of larger period $1/\delta$. This is exactly what is observed in TMV (Section 4). The dominant periodicity in the intensity along the layer-line enables us to determine r_0, the mean radius of the cylinder, while the positions of the zeros of the modulating function J_1, which show on the photographs as nodes, give the value of δ, the half-depth of the groove.

In principle, a further estimate of δ can be obtained by comparing the intensities

References p. 416.

on the third layer line with those on the equator. The 3rd layer-line intensity is, however, highly sensitive to the exact form of the groove. This is discussed in Section 6.

It is instructive to note that the innermost region of the third layer line is well described by the expression

$$\pi r_0 \delta J_1 (2\pi r_0 R) \tag{6}$$

obtained by introducing in expression (5) the approximation $J_1(x) \simeq \frac{1}{2}x$, which is valid for small values of x. This is the kind of expression that might be expected for a fluctuation in scattering density along a thin helix of radius corresponding to the outermost shell of the particle. The "strength" of the fluctuation is given by $\pi r_0 \delta$ which, for small values of δ, is equal to half the volume per unit length of the groove considered as having been scooped out of a cylinder of radius $r_0 + \delta$.

It is of interest to compare the above results with the diffraction pattern of a cylinder bearing a sinusoidal circular corrugation; that is, a cylinder whose radius varies periodically with z according to $r = r_0 + \delta \cos 2\pi z/P$. It may be shown (as in ref. 12) that on the layer line corresponding to the first order of the period P the transform is given to the second order in δ by

$$\pi r_0 \delta J_0 (2\pi r_0 R) \tag{7}$$

The expression (7) differs from (6) only in that the Bessel function of first order is replaced by one of zero order. This means that the diffraction pattern for a helical groove shows a shift away from the axis or meridian of the photograph, in contrast with that of a circular groove which does not. Thus here again the photographs of TMV leave us in little doubt that we are dealing with a structure having helical features.

(b) The second model which we shall consider is that of a helical groove of rectangular profile and of depth 2δ cut out of a cylinder of radius $r_0 + \delta$. This is illustrated in Fig. 3b where r_0, δ and P have the same meaning as before; but here there is another parameter, f, the fraction of a period occupied by the helical ridge.

The central cylindrical core of radius $r_0 - \delta$ contributes only to the equator, where its transform is

$$\pi(r_0 - \delta)^2 \frac{2 J_1 (2\pi[r_0 - \delta]R)}{2\pi R[r_0 - \delta]} \tag{8}$$

We may evaluate the transform of the residual helical ridge by regarding it as built up of a particular space-filling set of helices; the integration is easily effected by separation of co-ordinates. On the n^{th} layer line the transform is, per unit length of particle,

$$2\pi f \frac{\sin nf\pi}{nf\pi} \int_{r_0 - \delta}^{r_0 + \delta} J_n(2\pi r R)\, r\, \mathrm{d}r \tag{9}$$

On the equator ($n = 0$) this gives

$$f\left\{\pi(r_0 + \delta)^2 \frac{2 J_1 (2\pi[r_0 + \delta]R)}{2\pi(r_0 + \delta)R} - \pi(r_0 - \delta)^2 \frac{2 J_1 (2\pi[r_0 - \delta]R)}{2\pi[r_0 - \delta]R}\right\} \tag{10}$$

and to get the complete scattering function on the equator we must add the expressions

References p. 416.

(8) and (10). For the case $f = \frac{1}{2}$ when the ridge and groove each occupy half a period, the result is

$$\tfrac{1}{2}\left\{\pi(r_0+\delta)^2 \frac{2J_1(2\pi[r_0+\delta]R)}{2\pi[r_0+\delta]R} + \pi(r_0-\delta)^2 \frac{2J_1(2\pi[r_0-\delta]R)}{2\pi[r_0-\delta]R}\right\} \tag{11}$$

which we recognize as the mean of the transforms of two uniform cylinders of radii $r_0 + \delta$ and $r_0 - \delta$. In the innermost regions of reciprocal space this is identical with the transform of a cylinder of radius r_0. For higher values of R, the function will show a modulation of period $1/\delta$, just as does the transform of the quasi-sinusoidal groove (see expression (4)). However, we can see from the way in which (11) was derived as the sum of (8) and (10), that any departures from the ideal model (*e.g.* f different from $\frac{1}{2}$, or a difference of density between the ridge and the interior) will tend to mask the modulation.

The effect of the groove is most marked on the first layer line which corresponds to the third layer line for TMV. Here the transform is due only to the helical ridge (or groove) alone, and is given by

$$\begin{aligned} &2\pi f \frac{\sin \pi f}{\pi f} \int_{r_0-\delta}^{r_0+\delta} J_1(2\pi Rr)\, r\, \mathrm{d}r \\ &\quad = 2\pi f \frac{\sin \pi f}{\pi f}\left\{-\frac{1}{\pi R}\left[(r_0+\delta)J_0(2\pi[r_0+\delta]R) - (r_0-\delta)J_0(2\pi[r_0-\delta]R)\right]\right. \\ &\qquad \left. + \frac{1}{2\pi R^2}\int_{r-\delta}^{r_0+\delta} J_0(x)\,\mathrm{d}x\right\} \end{aligned} \tag{12}$$

The important terms here are the first two, and we see that the expression is essentially the difference of two oscillatory functions which have slightly different periods. It is clear that the result will have the form of a oscillatory function having the mean period $1/r_0$, modulated by a function with the larger period corresponding to the "beat frequency" $1/\delta$. Since this is precisely what we found for the quasi-sinusoidal groove, it is clear that this feature of the diffraction pattern is not sensitive to the exact form of the groove profile.

If δ is small compared with r_0, we may write down the approximation to (12) to the first order in δ. For $f = \frac{1}{2}$ we obtain

$$4 r_0 \delta J_1(2\pi R r_0) \tag{13}$$

which is of exactly the same form as the analogous expression (6) for the quasi-sinusoidal groove. The numerical factors in the two cases are somewhat different, as is to be expected, since it is the *average* not the *maximum* depth of the groove which determines the magnitude of the scattering function. These factors could be incorporated into a definition of *effective* depth of groove, but there is little point in pushing the theory so far.

Finally, for completeness we have also derived the transform of a cylinder bearing a circular corrugation of rectangular profile. It is, after subtracting the contribution of the central core,

$$f \frac{\sin \pi n f}{\pi n f}\left\{\pi(r_0+\delta)^2 \frac{2J_1(2\pi[r_0+\delta]R)}{2\pi[r_0+\delta]R} - \pi(r_0-\delta)^2 \frac{2J_1(2\pi[r_0-\delta]R)}{2\pi[r_0-\delta]R}\right\} \tag{14}$$

References p. 416.

per unit length of particle. Once again on the equator ($n = 0$) the result is identical with that for a helical groove of the same profile, but the higher layer lines differ in having true meridional maxima.

6 THE DEPTH AND NATURE OF THE GROOVE

Two independent methods by which the depth of a helical groove can be estimated from the X-ray diffraction data have been mentioned in the preceding section.

(a) The first method, based on a measurement of the positions of the zeros of the modulating function which operates on the 3rd layer-line (Fig. 2), gives directly the half-depth δ, of the groove, without making any assumption as to the mean radius of the particle. It has been shown that, for a groove of quasi-sinusoidal profile (Section 5a), this modulating function is of the form $J_1(2\pi\delta R)$. The 2nd and 3rd zeros of $J_1(2\pi\delta R)$ must therefore lie in the regions of zero intensity indicated by the arrows in Fig. 2. This condition is found to be fulfilled only if δ lies between 15.3 A and 16.3 A.

The modulating function for a groove of rectangular profile (Section 5b) is of closely similar form (whatever the value of f) ,and this model therefore leads to a value of δ closely similar to that given above.

(b) A further estimate of the depth of the groove can be obtained by comparing the *intensities* in the central regions of the equator and the 3rd layer-line. For this purpose, however, it is necessary to assume a particular form for the groove profile. The resulting value of δ will agree with that obtained by the first method (Section 6a) only if the correct groove profile is chosen.

The relative integrated intensities of the first non-origin peak on the equator and the first peak on the 3rd layer-line were determined from microdensitometer curves. The ratio of these intensities was then compared with the theoretical ratio, assuming various values of δ/r_0 and using the model of the quasi-sinusoidal groove profile (Section 5a). The theoretical intensity ratios were obtained by numerical integration, in the appropriate range, of the expressions

$$\int \left[J_0(2\pi\delta R)\,\frac{2J_1(2\pi r_0 R)}{2\pi r_0 R}\right]^2 \mathrm{d}R \qquad \text{for the equator}$$

and

$$\int \left[J_1(2\pi\delta R)\,\frac{2J_1(2\pi r_0 R)}{2\pi r_0 R}\right]^2 \mathrm{d}R \qquad \text{for the 3rd layer-line}$$

In this way, it was found that the observed and theoretical intensity ratios were equal for $\delta/r_0 = 0.88$. Assuming $r_0 = 75$ A, this gives $\delta = 6.6$ A.

Thus the value of δ obtained by this method, assuming a quasi-sinusoidal groove profile, is less than half that given by the period of the modulation function on the third layer-line. Now the period of the modulation function is approximately independent of the particular groove profile, (Section 5), and so it will provide the more reliable estimate of the groove depth. This means that the quasi-sinusoidal model does not give the intensity correctly. On the assumption of a rectangular groove having $f = \frac{1}{2}$, a similar discrepancy is found.

This substantial reduction in the strength of the groove effect, as compared with that which would be given by the above type of model in which groove and ridge have an equivalent diffracting power, may be attributed to one of three causes:

References p. 416.

(i) The density of the helical ridge which defines the groove may be less than that of the cylindrical core of the particle.

(ii) The helical ridge may be either considerably wider or considerably narrower than the groove which it defines. This corresponds to f very different from $\frac{1}{2}$, in the model of Section 5b.

(iii) The helical ridge may bear indentations or serrations or consist of a helical array of protuberances, and thus be of reduced weight.

The first explanation does not seem inherently probable. A choice between (ii) and (iii) cannot be made directly or on the basis of that part of the diffraction data considered in this section. However, some conclusions which have been drawn from other aspects of the X-ray diagrams appear relevant. We show below (Section 7) that in a close-packed assembly of TMV particles there is a high degree of interlocking, which must be attributed to the helical grooving. This excludes the possibility, under (ii), that the ridge may be wider than the groove, but leaves open the possibility of a ridge narrower than the groove.

The third possibility presents an attractive picture if we assume that each protein sub-unit is of such a shape as to give a protuberance at the surface of the particle. This leads directly to a helical array of protuberances, the helix having the required parameters.

7. THE 3RD LAYER-LINE IN X-RAY DIAGRAMS OF WET AND DRY TMV

One of the most striking differences between the X-ray diagrams of wet and dry TMV preparations lies in the central region of the 3rd layer-line. The wet material shows two very strong maxima close to the axis on the 3rd layer-line, having R-values corresponding to about 270 A and 99 A. In dry specimens however, the first of these is entirely absent; only a weaker and more diffuse peak having an R-value corresponding to approximately 100 A is observed (see Fig. 6 of preceding paper). In the best-orientated dry specimens, this peak is seen to be resolved into two peaks with R-values corresponding to approximately 130 A and 75 A respectively.

This modification of the central region of the 3rd layer-line is observed not only in strongly dried TMV, but also in dried specimens subsequently maintained in an atmosphere of relative humidity 75% or 92%. At these relative humidities the outer regions of the 3rd layer-line (and of other layer-lines) are closely similar to those given by orientated gel preparations.

It is hard to see how the presence or absence of the central maxima on the 3rd layer-line could depend simply on the amount of water surrounding cylindrical particles. If we assume, on the other hand, that the particles are helically grooved, a satisfactory explanation of the observed change is readily available.

When parallel rods bearing similar helical grooves are brought into contact with one another, they will, in general, interlock. The smaller the tilt of the helix, the greater will be the degree of interlocking. A close-packed array of such grooved rods can be assembled in which interlocking occurs between *all* pairs of nearest neighbours. This is illustrated in Fig. 4, which shows seven helically grooved rods fully interlocked. The central rod can (with the aid of a screw-driver) be screwed in and out among its six neighbours without altering the packing of the rods.

We shall now show that, if dry, orientated TMV particles pack with their grooves

References p. 416.

interlocked in this way, the modification of the central region of the 3rd layer-line is explained.

Imagine the model of Fig. 4 to be extended in all directions; that is, suppose the close-packed, uniform-density, interlocking rods to be both numerous and long. We then have a model of a *truly crystalline* structure, with a hexagonal unit cell in which a is the inter-rod distance (or twice the packing radius, r_1) and c the pitch of the helical groove. Screwing one of the rods in or out with respect to its neighbours will not destroy the crystallininity of the arrangement.

Suppose, now, that the uniform-density rods of Fig. 4 are replaced by rods having an internal structure such that it can be described as the sum of a number of coaxial, *smooth*, thin helices of different weight, radius and azimuth but equal pitch, the pitch being equal to the pitch of the groove. In this case, also, the fully interlocked array of rods is perfectly crystalline: screwing one of them in or out with respect to its neighbours makes no difference to the crystallinity.

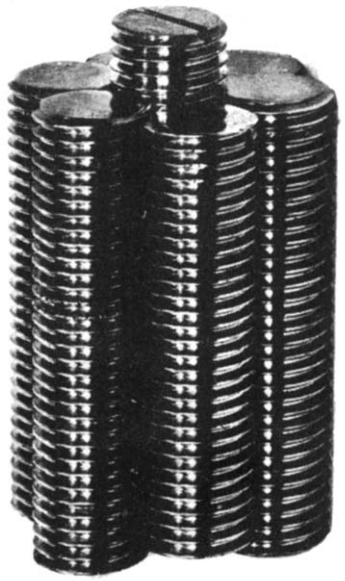

Fig. 4. A model to illustrate a portion of the close-packed array formed by helically grooved rods when fully interlocked. The central rod in the model can be screwed in and out by means of a screw-driver. It is suggested that in dry TMV the particles pack in this way.

It is only when the smooth, thin, constituent helices of this model are replaced by constituent helices which are discontinuous, as in a real molecular structure, that the crystallinity of the assembly of interlocking rods is destroyed. In this case, the movement involved in screwing one rod in or out with respect to its neighbours alters the relative positions of the *atoms* in neighbouring rods. However, we have shown (Section 2) that there is a part of the X-ray fibre-diagram which is unchanged when a structure built up of smooth helices is replaced by one built up of discontinuous helices bearing equally spaced point-scatterers, or atoms. For TMV, this part is the contribution of Bessel function of order n to the layer-lines $3n$; that is, the central regions of layer-lines 3, 6, 9 *etc.* We must therefore expect that, as far as this part of the diagram is concerned, diffraction by a dry, fully interlocked assembly of helically grooved TMV particles will resemble diffraction by a crystal.

Now diffraction by a crystal differs from that of an assembly of dispersed virus particles in random rotation about their long axes in that, whereas the latter shows the *continuous* Fourier transform of the particle on each layer-line, the former shows only a sampling of the transform at the points of the reciprocal lattice of the crystal. In the outer regions of the layer-lines, the reciprocal lattice points will be crowded together, and the sampled transform will be indistinguishable from the continuous transform. There will, however, be a region in the centre of each layer-line in which diffraction may be significantly different in the two cases.

We shall consider only the central region of the 3rd layer-line. This, as has been

References p. 416.

shown above, is determined predominantly by a contribution $J_1(2\pi r_0 R)$, where r_0 is the mean radius of the particle, and equal to approximately 75 A.

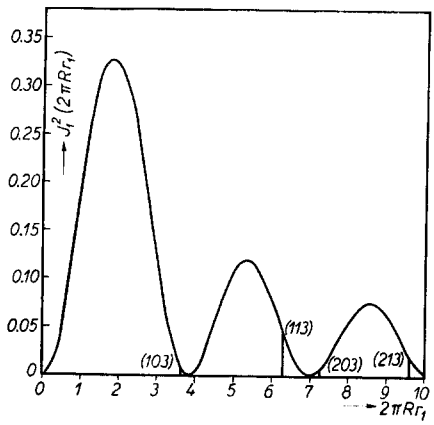

Fig. 5. The 3rd layer-line in X-ray diagrams of TMV. The curve is a plot of $[J_1^2(2\pi r_1 R)]$, the intensity to be expected near the meridian for helically grooved rods of mean radius r_1 dispersed as in a gel. The vertical lines represent the positions of the reflections for the pseudo-crystalline close-packed array formed by such rods when fully interlocked; the hexagonal unit cell has a side of length $2r_1$. This shows why the strong first peak on the 3rd layer-line of TMV gels disappears in dry specimens. Note that the effect is independent of the value of r_1.

If the depth of the groove is small, or if its contour is such as to permit a high degree of interlocking, the packing radius, r_1, will be approximately equal to the mean radius, r_0. The amplitude of the reflections of the pseudo-crystalline array of close-packed virus particles in which the hexagonal unit cell has $a = 2r_1$ will therefore be given, in the region considered here, by the appropriate values of the structure factor of a helically grooved rod having $r_0 = r_1$; that is, by the appropriate values of $J_1(2\pi r_1 R)$ (with $r_1 = 75$ A).

In Fig. 5 $J_1^2(2\pi r_1 R)$ is plotted as a function of $2\pi r_1 R$, and the positions and amplitudes of the first four reciprocal lattice points of a hexagonal unit cell having $a = 2r_1$ are indicated. It is immediately clear why the strong first maximum in the structure factor of the 3rd layer-line (i.e. the first band of $J_1^2(2\pi r_1 R)$) is absent in the diffraction pattern of dry TMV. The only lattice reflection of the pseudo-crystalline array of helically grooved particles which falls within this band is the (103) (corresponding to the (101) reflection of the model of Fig. 4), and this lies very close to its outer edge. The first observed reflection for the dry material is therefore both displaced and weak. The intensity of the (113) reflection which falls in the second band of $J_1^2(2\pi r_1 R)$ is rather higher. The maxima observed at approximately 130 A and 75 A on the 3rd layer-line of well-orientated dry TMV thus correspond well with the (103) and (113) reflections of a pseudo-crystalline array of virus particles of packing radius 75 A.

DISCUSSION

In the preceding sections the nature of the helical groove on the TMV particle has been discussed with reference to the mild (U2) strain. The existence of the groove was, however, first suggested by the appearance of the Patterson map for a normal strain[5]. Moreover, all strains of TMV so far examined, as well as cucumber virus 4, show a large period modulation of the 3rd layer-line[13] and also the same kind of intensity changes in this layer-line in passing from the gel to the dry state. We may therefore assume that the groove is present in all strains and has the same depth of approximately 30 A. However, the modulation function is more strongly defined in the photographs of U2 than in those of other strains, and suggests that in this strain the groove is more highly developed than in the others. There is also some evidence[14] that the packing radius of U2 is slightly smaller than that of other strains, which

References p. 416.

suggests that the form of the groove is such as to allow a higher degree of interlocking between neighbouring particles.

The observation that the helical grooves and ridges of two (or more) TMV particles can interlock with one another to a considerable extent imposes certain important limitations on the possible forms of the groove contour. In particular, the helical ridge obviously cannot be more bulky than the groove which it defines. The measurements on the 3rd layer-line of the intensity of diffraction by the groove (Section 6), considered in conjunction with the interlocking effect, indicate that the "weight" of the groove is about twice that of the ridge. Although other possibilities cannot be definitely excluded, the most plausible explanation of this seems to be that the ridge, in reality, consists of a helical array of protuberances, one for each protein sub-unit. Both the helical groove and the discontinuity of the ridge which defines it are then simply the consequence of the shape of the individual sub-units which constitute the virus protein.

When TMV protein is depolymerised to a molecular weight of about 100,000, the RNA content of the virus extracted, and the protein repolymerised[15], the resulting RNA-free rods, which have the same diameter as TMV particles, show also, the same small-period oscillation of intensity on the 3rd layer-line and the same large-period modulation of it[16]. This provides further proof that the helical groove, whatever form it may take, is an inherent property of the protein part of the virus.

Since the virus protein can be broken down into a low molecular-weight material and then, readily and reversibly, repolymerised into TMV-like particles[15,16], the virus sub-units, or at least small groups of such sub-units, must be capable of independent existence in a form in which the configuration of the polypeptide chains does not differ greatly from that in the virus. If the shape of the sub-units were such that, when polymerised, they filled completely a perfect cylindrical volume (with the exception of a central core for the virus RNA[4,7,8]), the shape of each sub-unit would be approximately that of a truncated wedge. This is not a particularly probable shape for a low molecular-weight protein molecule. In the structural model proposed in this paper the outer regions of the cylindrical volume are incompletely filled, and the shape of the protein molecule appears more reasonable.

A further consequence of the model is that the virus particle will have a rather large surface area. It may well be as much as twice that of a smooth cylinder of the same radius. This means that a substantial fraction of the protein will lie near the surface, and may well explain the extensive chemical reactions which can be carried out on intact TMV particles[17].

ACKNOWLEDGMENTS

We wish to thank Professor J. D. BERNAL for his interest and encouragement, Dr. P. M. B. WALKER (M.R.C. Biophysics Unit, King's College London) for the use of a microdensitometer, and the Agricultural Research Council (R.E.F.) and the Nuffield Foundation (A.K.) for financial support.

References p. 416.

SUMMARY

It is shown that various aspects of the X-ray fibre-diagrams of TMV can be explained by the presence of some form of helical groove (with its resulting helical ridge) on the surface of the virus particle. The groove follows the line of the main protein helix (pitch 23 A) and is approximately 30 A in depth. The form of the groove and ridge is such as to permit a high degree of interlocking between neighbouring particles, and it is suggested that the ridge may in fact consist of a series of protuberances, one corresponding to each protein sub-unit.

As a result, the surface area of the virus particle must be considerably greater than that of a smooth cylinder of the same diameter, and this may be important in determining the chemical properties of the intact virus.

RÉSUMÉ

Les auteurs montrent que différents aspects des diagrammes de fibre aux rayons X du TMV peuvent s'expliquer par la présence d'une certaine forme de rainure hélicoïdale (avec sa crête hélicoïdale résultante) à la surface de la particule de virus. La rainure suit la ligne de l'hélice protéique principale (pas 23 A) et a une profondeur de 30 A environ. La forme de la rainure et de la crête est telle qu'elle permet un degré élevé d'interpénétration entre particules voisines, et les auteurs suggèrent que la crête peut en fait être constituée d'une série de protubérances, chacune correspondant à une sub-unité protéique.

Il en résulte que l'aire de la surface de la particule de virus doit être considérablement plus grande que celle d'un cylindre lisse de même diamètre; cette conformation peut jouer un rôle important dans la détermination des propriétés chimiques du virus intact.

ZUSAMMENFASSUNG

Es wird bewiesen, dass verschiedene Aspekte der TMV-Röntgen-Faserdiagramme durch die Anwesenheit einer Art von Schraubenrinne (mit der sich daraus ergebenden Schraubenkannte) auf der Viruspartikeloberfläche erklärt werden können. Die Rinne folgt der Linie der Hauptproteinschraube (Steighöhe 23 A); ihre Tiefe ist ungefähr 30 A. Die Form von Rinne und Kante ermöglicht einen hohen Verflechtungsgrad der Nachbarpartikeln; die Annahme wird befürwortet, dass die Kante aus einer Reihe von Auswüchsen bestehen könnte, deren jeder einer Proteinsubeinheit entsprechen würde. Die Viruspartikeloberfläche muss daher bedeutend grösser sein als diejenige eines glatten Zylinders mit dem gleichen Durchmesser. Dies kann bei Bestimmung der chemischen Eigenschaften des intakten Virus von Wichtigkeit sein.

REFERENCES

[1] J. D. BERNAL AND I. FANKUCHEN, *J. Gen. Physiol.*, 25 (1941) 111.
[2] R. C. WILLIAMS AND R. L. STEERE, *J. Am. Chem. Soc.*, 73 (1951) 2057.
[3] R. C. WILLIAMS, *Biochim. Biophys. Acta*, 8 (1952) 227.
[4] J. D. WATSON, *Biochim. Biophys. Acta*, 13 (1954) 10.
[5] R. E. FRANKLIN, *Nature*, 175 (1955) 379.
[6] R. E. FRANKLIN AND A. KLUG, *Acta Cryst.*, 8 (1955) 777.
[7] G. SCHRAMM, G. SCHUMACHER AND W. ZILLIG, *Nature*, 175 (1955) 549.
[8] R. G. HART, *Proc. Natl. Acad. Sci. U.S.*, 41 (1955) 261.
[9] W. COCHRAN, F. H. C. CRICK AND V. VAND, *Acta Cryst.*, 5 (1952) 581; F. H. C. CRICK, *Thesis*, Cambridge, 1953.
[10] A. SIEGEL AND S. G. WILDMAN, *Phytopathology*, 44 (1954) 277.
[11] P. P. EWALD, *Proc. Phys. Soc. London*, 52 (1940) 167.
[12] R. S. BEAR AND O. E. A. BOLDUAN, *Acta Cryst.*, 3 (1950) 236.
[13] R. E. FRANKLIN, *Biochim. Biophys. Acta*, 19 (1956) 203.
[14] J. T. FINCH, unpublished.
[15] G. SCHRAMM, *Z. Naturforsch.*, 26 (1947), 112 and 249.
[16] R. E. FRANKLIN, *Biochim. Biophys. Acta*, 18 (1955) 313.
[17] M. L. ANSON AND W. M. STANLEY, *J. Gen. Physiol.*, 24 (1941) 269; G. L. MILLER AND W. M. STANLEY, *J. Biol. Chem.*, 146 (1942) 331; C. A. KNIGHT, *J. Biol. Chem.*, 192 (1951) 727.

Received July 15th, 1955